

Chapter 7

Plumes and hotspots

Apart from plate tectonics, another type of dynamics is probably present in the Earth mantle in the form of mantle plumes. Plumes are blobs of material that go unstable at a thermal boundary layer, and then departure towards the opposite boundary. In principle both hot upwelling plumes and cold downwelling plumes can exist in a fluid. But since the rheology of the Earth is strongly temperature-dependent, the cold downwellings appear in sheet-like shape (i.e. slabs).

The main indication for plumes comes from the existence of *hotspots*, which are areas of intra-plate volcanism. These hotspots seem to move relative to the plate on which they appear, resulting in *hotspot tracks*, linear volcanic island chains, of which the Hawaii-Emperor chain is the most famous one. Morgan [1971] was the first to recognize that these hotspots are the result of mantle plumes that are almost fixed with respect to each other. Laboratory and numerical studies have been performed to examine the appearance of a mantle plume. Plume material is hotter, and therefore less buoyant, and less viscous than the surrounding mantle material with a ‘normal’ temperature. Plumes usually consist of a *head* and a *tail*, as indicated in Figure 7.1.

In [Turcotte and Schubert, 2002], an analysis of the size and dynamics of a plume is described, based on an analytical description for both the plume head and tail. The plume head can be regarded as a low-viscous, buoyant sphere that rises through a more viscous, denser fluid. For such a rising-sphere scenario, an analytical solution for the rising velocity exists (the so called Stokes velocity for rising spheres in an infinite viscous fluid) [Turcotte and Schubert, 2002]

$$U = \frac{r^2 g (\rho_m - \rho_p)}{3\eta_m} \quad (7.1)$$

with r the radius of the sphere, ρ_m and η_m the mantle density and viscosity, and ρ_p the viscosity inside the sphere. The plume tail can be regarded as upwelling material through a cylinder, for which an analytical solution for the volume flux Q_p can also easily be obtained [Turcotte and Schubert, 2002]:

$$Q_p = \frac{\pi(\rho_m - \rho_p)gR^4}{8\eta_p} \quad (7.2)$$

with η_p the viscosity of the material inside the plume tail, and R the radius of the tail. Using $\rho = \rho_0(1 - \alpha(T - T_0))$, we can relate the density difference to a temperature difference between inside and outside the plume head and tail. The *buoyancy flux* $B = Q_p(\rho_m - \rho_p)$ is defined as the volume flux times the density difference. Furthermore, a *plume heat flux* $Q_H = \rho_m c_p (T_p - T_m) Q_p$ can be defined as the amount of heat carried up through a horizontal interface per unit of time, in which c_p is the specific heat, and T_p and T_m the plume and mantle temperature, respectively.

The primary information on the size or strength of a plume comes from an estimate of the buoyancy flux: as a plume impinges on the surface, the plume buoyancy will lift up this surface a bit. After the plume head has reached the surface, new plume material is continuously delivered by the tail of the plume. This material is dragged along sideways by the plate that moves with respect to the plume location. Figure 7.2 from [Davies, 1999] explains this feature. Assuming local isostasy, the plume buoyancy flux B can be related to the (integrated) swell topography as [Turcotte and Schubert, 2002]:

$$B = (\rho_m - \rho_w) A_s u_p \quad (7.3)$$

with ρ_w the water density, A_s the cross-sectional area of the swell in a vertical cross-section perpendicular to the hotspot track, and u_p the plate motion relative to the plume. Davies [1988] and Sleep [1990] calculated the

buoyancy fluxes of the most important hotspots on Earth by measuring A_s and u_p . As an example, we discuss the Hawaiian hotspot, again taken from [Turcotte and Schubert, 2002]: there A_s was measured to be 1.13 km^2 . With $u_p = 9 \text{ cm/yr}$, $\rho_m = 3300$ and $\rho_w = 1000 \text{ kg/m}^3$ gives $B = 7400 \text{ kg/s}$. With $C_p = 1.25 \text{ kJ/kg,K}$ and $\alpha = 3 \times 10^{-5} \text{ 1/K}$, this gives a plume heat flux $Q_H = 3 \times 10^{11} \text{ W}$, almost 1% of the Earth's total heat flux. With a plume viscosity $\eta_p = 10^{19} \text{ Pa s}$, and a plume excess temperature of 200 K, this gives a plume radius of 84 km. A volume flux of approximately $12 \text{ kg}^3 \text{ m}^{-3}$ can be found, which is about 100 times the amount of basalt found in a similar cross section. Basalt is the result of partial melting of the hot plume material, so this analysis suggests that about 1% of the plume material is melted during its ascend to the surface. If one assumes that the plume head rises with the same speed as the average velocity in the plume tail, we find

$$Q_p = \pi R^2 U \quad (7.4)$$

which suggests that the Hawaiian plume head and material in the trailing tail rises with a speed of 54 cm/yr, much faster than plate velocities.

So the continuous rising and melting of plume material from its tail can be related to a hotspot track, and swell. The arrival of the voluminous plume head at the base of the lithosphere leads to excessive volcanism, which is observed as continental or oceanic flood basalt provinces. Continental flood basalts are also called *traps*, of which the Deccan Traps are the most famous. In oceanic lithosphere, such flood basalts are called large igneous provinces (or LIPs), of which Ontong-Java is the largest one. In some cases we can trace back the hotspot track to its beginning at a flood basalt. A classical example is the Deccan Traps, followed by the hotspot track leading to the Réunion hotspot in the Indian Ocean. Figure 7.3 shows a compilation of traps, LIPs and hotspots with their tracks from [Duncan and Richards, 1991]. Taking $B = 1.4 \times 10^3 \text{ kg/s}$ for the Réunion plume, and a mantle viscosity of 10^{21} Pa s gives a plume head with a radius $r = 336 \text{ km}$, and a volume of $1.2 \times 10^8 \text{ km}^3$. The basalt volume of the Deccan Traps is about $1.5 \times 10^6 \text{ km}^3$, which indicates again that about 1% of the plume material is melted.



Figure 7.1: Photograph of a low-density, low-viscosity glucose fluid plume ascending in a high-density, high-viscosity glucose fluid [from Olson and Singer, 1985].

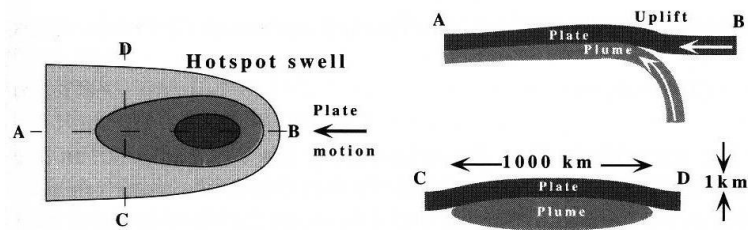


Figure 7.2: Sketch of a 3-D hotspot swell. Left: contourplot of the swell topography. Right: two vertical cross-sections of the plume and swell. From [Davies, 1999].

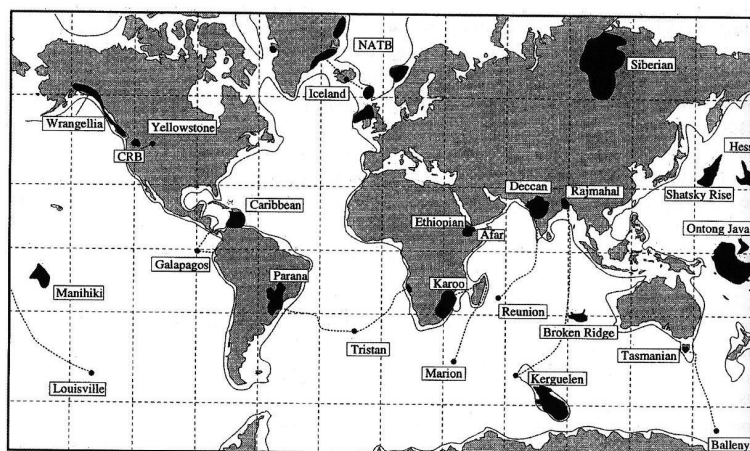


Figure 7.3: Map of LIPs, traps, and hotspots. Dotted lines are the hotspot tracks. From [Duncan and Richards, 1991].

Bibliography

- G. F. Davies. *Dynamic Earth: Plates, Plumes and Mantle Convection*. Cambridge University Press, Cambridge, 1999.
- G.F. Davies. Ocean bathymetry and mantle convection. 1. Large scale flow and hotspots. *Journal of Geophysical Research*, 93:10467–10480, 1988.
- R. Duncan and M.A. Richards. Hotspots, mantle plumes, flood basalts, and true polar wander. *Reviews of Geophysics*, 29:31–50, 1991.
- W. J. Morgan. Convection plumes in lower mantle. *Nature*, 230(5288):42–, 1971. NATURE.
- P. Olson and H. Singer. Creeping plumes. *Journal of Fluid Mechanics*, 158(SEP):511–531, 1985. J FLUID MECH.
- N. Sleep. Hotspots and mantle plumes: some phenomenology. *Journal of Geophysical Research*, 95:6715–6736, 1990.
- D. L. Turcotte and G. Schubert. *Geodynamics*. Wiley, 2nd edition, 2002.